INTERNATIONAL TABLES FOR CRYSTALLOGRAPHY

ISSN 1574-8707
it.iucr.org

Volume I, X-ray Absorption Spectroscopy and Related Techniques
ISBN: 978-1-119-43394-1

Chapter 5.1

Received 24 October 2016
Accepted 26 June 2019

Keywords: background removal; EXAFS.

Background removal

Matthew Newville*

Center for Advanced Radiation Sources, The University of Chicago, Chicago, IL 60637, USA. *Correspondence e-mail: newville@cars.uchicago.edu

In order to perform a structural analysis of extended X-ray absorption fine-structure (EXAFS) data, the fine structure must be extracted from the measured absorption coefficient $\mu(E)$. The EXAFS or differential absorption $\chi(E)$ is commonly defined as $[\mu(E) - \mu_0(E)]/\mu_0(E)$, where $\mu_0(E)$ is a smooth function of energy E representing the absorption from the idealized isolated absorbing atom. Unfortunately, it is not always easy to distinguish which parts of $\mu(E)$ are due to structurally derived EXAFS and which parts are due to the atomic or electronic excitations that comprise $\mu_0(E)$. If not performed carefully, the removal of the 'background' $\mu_0(E)$ can significantly impact the EXAFS oscillations in $\chi(E)$ and the results of the structural analysis. The details of mathematical determination of the EXAFS background $\mu_0(E)$ are discussed and examples are given to illustrate the common strategies for background removal of EXAFS data.

1. The EXAFS background $\mu_0(E)$

All theories for extended X-ray absorption fine structure (EXAFS) and essentially all approaches to the quantitative analysis of EXAFS data to determine local atomic structure use the EXAFS χ function, the *fine structure* in the absorption coefficient. This fine structure χ is not directly measured and must be extracted from measurements of the absorption coefficient $\mu(E)$. With the EXAFS being a differential signal, χ is typically defined by

$$\mu(E) = \mu_0(E)[1 + \chi(E)], \tag{1}$$

where $\chi(E)$ is the EXAFS, containing the structural information, and $\mu_0(E)$ is a background signal. This background is often described as 'the smooth atomic background', which might suggest that this represents the absorption by an isolated atom, say in the gas phase. In addition to being impractical to measure for many atoms, the absorption of an isolated atom would miss many of the electronic and chemical effects that occur in most EXAFS spectra, including chemical shifts due to changes in oxidation state. More accurately, the background $\mu_0(E)$ represents the absorption by an idealized excited atom in the electronic environment of its solid or molecule form, but without the photoelectron scattering that gives rise to the EXAFS. Put most simply, $\mu_0(E)$ is the part of the absorption that does not contain the EXAFS.

Although it is not necessarily difficult to separate $\mu(E)$ into $\mu_0(E)$ and $\chi(E)$, this process should be done with care. If performed improperly this data-reduction step can adversely affect the resulting χ and the structural parameters derived from it. Strategies for avoiding such problems will be discussed later in this chapter.

The background-subtraction process is often tied closely to the subtraction of a pre-edge baseline and determination of

Related chapters

Volume I: 3.14, 3.43, 4.6, 4.7, 5.2, 5.3, 5.6, 5.7

the edge step, which are discussed elsewhere in this volume (Webb, 2024). This close tie is at least partly because most EXAFS measurements focus on accurate measurements of the relative absorption from a sample but do not attempt to make an accurate absolute measurement of the total mass attenuation coefficient or absorption coefficient. In particular, simple ratios of detector intensities such as those from gas-filled ion chambers are typically used to represent $\mu(E)$ [or at least $t\mu(E)$ for average sample thickness t]. These intensities may have scaling and offset factors, and may drift noticeably with energy. Such energy drifts are not especially noticeable for EXAFS measured in transmission mode with ion chambers filled with comparable gases, but can be large for EXAFS measured in fluorescence mode, where the energy response of the fluorescence detector is much different from that of an ion chamber sampling the incident beam. In short, the expected E^{-3} dependence of $\mu(E)$ may not be reflected in the data presented as 'raw' $\mu(E)$ data, especially for data measured in fluorescence. This means that applying a naive reading of the above formula

$$\chi(E) = \frac{\mu(E)}{\mu_0(E)} - 1 = \frac{\mu(E) - \mu_0(E)}{\mu_0(E)} \qquad (2)$$

may lead to unstable values of $\chi(E)$. On the other hand, if one uses background-subtracted and properly normalized experimental data for $\mu(E)$, such that $\mu(E)$ has a value near 0 below the absorption edge and a value near 1 above it, then this definition reduces to

$$\chi(E) = \mu_{\rm norm}(E) - \mu_{\rm norm_0}(E) = \frac{\mu(E) - \mu_0(E)}{\Delta\mu}, \qquad (3)$$

where $\mu_{\rm norm}(E)$ is the pre-edge-subtracted, edge-step normalized $\mu(E)$, $\Delta\mu$ is the edge step found in the normalization step and $\mu(E)$ now represents the pre-edge-subtracted $\mu(E)$.

While this approach of using edge-step normalized $\mu(E)$ ignores the expected energy decay of the true absorption coefficient, it recognizes a few practical realities of experimental EXAFS measurements. Firstly, the decay in $\mu(E)$ is expected to be small for the 1000 eV or so energy range of most EXAFS measurements. Secondly, the intensity measurements that are used to construct a spectrum with the fine structure of $\mu(E)$ may have energy drifts that far exceed the true decay in $\mu(E)$. Thirdly, the small correction to χ needed to account for the expected decay of $\mu(E)$ mostly affects the amplitude and specifically tends to give a constant offset in the absolute value of σ^2, which is often of secondary importance in structural analysis.

Most theoretical and analytical treatments of EXAFS refer to the wavenumber of the photoelectron k instead of the energy of the absorbed X-ray E, and the conversion from E to k is often included in the background-subtraction step. This is performed with the simple relation $k = [2m(E - E_0)/\hbar^2]^{1/2}$, where m is the electron mass and $\hbar$ is Planck's constant, and E_0 is the estimated threshold energy. Thus, it is typical to consider background subtraction as determining $\mu_0(E)$ in order to extract $\chi(k)$ from an experimentally measured spectrum of $\mu(E)$ for further analysis.

2. Approximating $\mu_0(E)$ with a spline

Since $\mu_0(E)$ cannot be measured independently, it is determined empirically for each spectrum. Although approaches using progressive smoothing or simple polynomials fitted to the measured $\mu(E)$ have been used in the past, nearly all background estimations currently in use rely on piecewise polynomials or *spline* functions, typically cubic splines or B-splines (deBoor, 1978). The principal characteristic of a spline is that it has a continuous value and first derivative in the independent variable (for EXAFS, E), but can have a small number of *breakpoints* or *knots* which may have a discontinuity in higher derivatives. The shape of the spline can then be controlled by the number and energy values of these knots, with the intensity (or μ values) of the knots adjusted until a satisfactory result is found.

Of course, with a sufficient number of knots, all of the fine structure in $\mu(E)$ could be followed, which is clearly undesirable for separating $\mu_0(E)$ and $\chi(E)$. To control the stiffness of the spline, we must determine how to limit the number of knots to use. In addition, we must decide which μ values for each knot are more satisfactory. Fortunately, the Fourier analysis that is central to EXAFS can aid both of these decisions (Cook & Sayers, 1981). The qualitative description of $\mu_0(E)$ as *the slowly varying* part of $\mu(E)$ suggests that the knots in $\mu_0(E)$ should be adjusted to match only the low-R parts of the spectrum, leaving the higher R parts of $\mu(E)$ to give $\chi(k)$. This observation can be made quantitative with a single physical parameter $R_{\rm bkg}$ that is the distance separating the spectrum μ into background μ_0 and EXAFS signal χ. Since atoms are typically separated by at least 1.5 Å, a rule of thumb is to set $R_{\rm bkg}$ to 1.0 Å or half the near-neighbour distance, although the precise value used may need adjustment for each system.

In addition to having an R value to separate $\mu_0(E)$ from $\chi(E)$, we can select how many knots to use with a modification of the Nyquist–Shannon sampling theorem (Shannon, 1949; Stern, 1993) that says there are

$$N \simeq \frac{2\Delta k \Delta R}{\pi} + 1 \qquad (4)$$

independent measurements in an EXAFS spectrum that extends over a k-range and R-range of Δk and ΔR. Thus, for a spectrum with k-range Δk, we need approximately

$$N_{\rm bkg} = \frac{2\Delta k R_{\rm bkg}}{\pi} + 1 \qquad (5)$$

knots to represent $\mu_0(E)$ (Newville *et al.*, 1993). This view also suggest that the energies of the knots should be evenly spaced in k so as to best use the amount of information about the low-R components of the spectrum.

To determine $\mu_0(E)$ for a spectrum, a least-squares fit (see Newville, 2024) can be used. In this process, the $N_{\rm bkg}$ energies for the knots points are selected, and the y (that is, μ) values

for these knots are assigned [initially to the nearest $\mu(E)$ value] and used to generate a candidate spline for $\mu_0(E)$ at all energies. This candidate $\mu_0(E)$ is subtracted from the data $\mu(E)$ to give a candidate $\chi(k)$, which is then Fourier transformed to $\chi(R)$, where only the components below $R_{\rm bkg}$ are kept. The $N_{\rm bkg}$ values for the y coordinates of the spline knots are then adjusted until the components resulting in $\chi(R)$ below $R_{\rm bkg}$ are minimized in the least-squares sense. These optimal values for the $N_{\rm bkg}$ values of the knots then fully define $\mu_0(E)$. With $N_{\rm bkg}$ typically ranging from 5 to 20 and good initial values for the spline knots coming from the input $\mu(E)$, this procedure is remarkably robust and efficient. Because it looks only at the low-R components of the $\mu(E)$ signal, there is little chance that the resulting spline can match any part of the real EXAFS signal above $R_{\rm bkg}$. It should also be noted that this fit can use uncertainties in the measured $\mu(E)$ to better determine the results and can provide uncertainties in both the derived $\mu_0(E)$ and $\chi(k)$ functions.

To illustrate these background-removal concepts, we show the results for the background and the resulting $\chi(k)$ and $\chi(R)$ for the Ni K-edge spectrum of NiS_x, which has a near-neighbour distance around 2.3 Å. Fig. 1 shows three copies of the normalized experimental $\mu(E)$ data with $\mu_0(E)$ determined with $R_{\rm bkg}$ values of 0.2, 1.2 and 2.2 Å. Figs. 2 and 3 show the resulting k-weighted $\chi(k)$ and $|\chi(R)|$ for these values of $R_{\rm bkg}$.

As can be seen from this example, the $\mu_0(E)$ for $R_{\rm bkg}$ = 2.2 Å follows the EXAFS oscillations too closely, effectively erasing the first-shell EXAFS that peaks around 1.9 Å. Using $R_{\rm bkg}$ = 0.2 Å results in a $\mu_0(E)$ that goes through the oscillations in $\mu(E)$ but appears to be too stiff, giving a $\chi(k)$ that still has slow variation with k and $\chi(R)$, with a large peak around 0.2 Å, far below the peak for the first shell. With $R_{\rm bkg}$ = 1.2 Å, the slow variations in $\mu(E)$ are followed well by $\mu_0(E)$ without following the EXAFS oscillations themselves, $\chi(k)$ oscillates uniformly around the origin and most of the non-EXAFS signal at low R that is present for $R_{\rm bkg}$ = 0.2 Å is now smooth like a rhapsody (Dylan, 1971). It is also apparent that the first-shell EXAFS is largely unchanged between the spectra extracted with $R_{\rm bkg}$ of 0.2 and 1.2 Å. This illustrates the point that the R components of the EXAFS are largely independent and suggests that peaks at low R for the stiffer spline should not have a substantial impact on the EXAFS or on results from analyzing EXAFS with imperfect background removal. However, the spectrum shown here has a rather large near-neighbour distance and the relatively heavy scatterer sulfur. For shorter neighbour distances and light scatterers (C, O and N, for example), the shape of the first peak is more asymmetric and skewed to lower R. For these cases, and for spectra with strong white lines, obtaining a good background that does not alter the first shell can be somewhat trickier. Generally speaking, erring on the side of shorter $R_{\rm bkg}$ should be preferred.

A slight improvement can be made for multiple spectra or for well characterized systems by using a 'known' or even a theoretical $\chi(k)$ that is expected to be close to $\chi(k)$ for the unknown spectrum. Here, the Fourier transformed 'standard' $\chi(k)$ can be used to model the expected spectral leakage from the EXAFS single into the low-R part of the spectrum. This gives a very small change in the mathematical process, now minimizing the difference between the candidate $\chi(R)$ and the 'standard' $\chi(R)$ below $R_{\rm bkg}$ instead of simply minimizing the

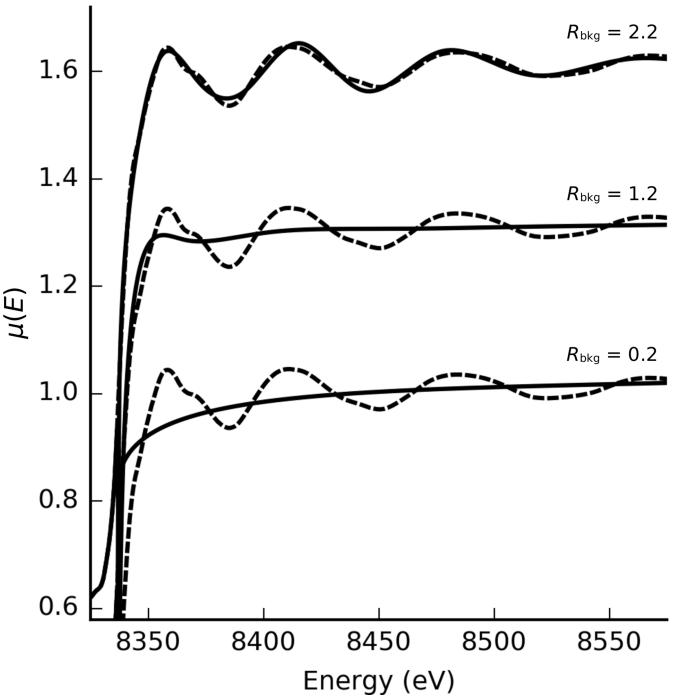

Figure 1
Background subtraction and the effect of $R_{\rm bkg}$. Experimental Ni K-edge $\mu(E)$ for NiS_x are shown (dashed lines) with background $\mu(E)$ found using $R_{\rm bkg}$ of 0.2, 1.2 and 2.2 Å (solid lines).

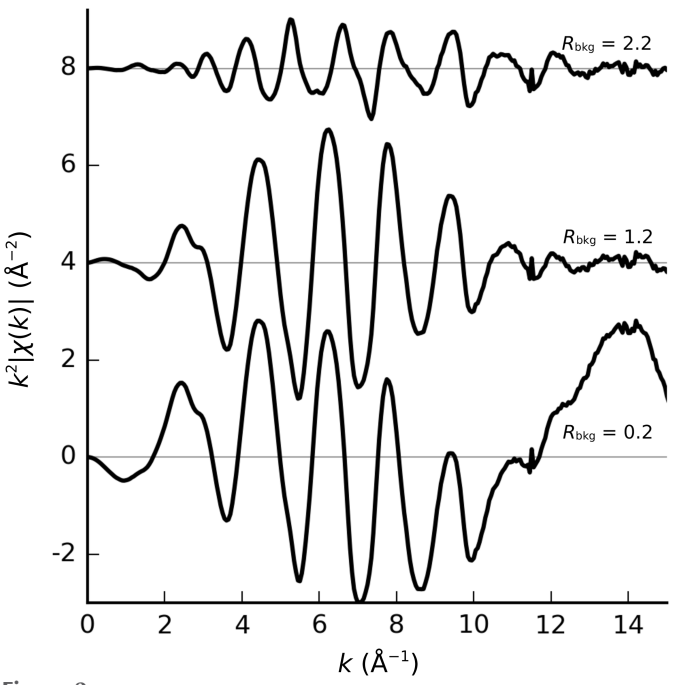

Figure 2
The resulting k-weighted $\chi(k)$ for the NiS_x EXAFS spectrum using $R_{\rm bkg}$ of 0.2, 1.2 and 2.2 Å.

value of $\chi(R)$. The improvements made by using such a standard can be most profound for shorter neighbour distances and light scatterers, including the important case of metal–oxygen bonds. To be clear, this use of a standard to assist in background removal does bias the result somewhat towards matching the ligand of the standard, but the first-shell ligand is often known ahead of time and can be corroborated by inspection of the XANES.

Since this approach uses only the low-R components of $\mu(E)$, there are very few restrictions on the energy values for $\mu_0(E)$. Without other information there is little to prevent a spline from diverging from the measured $\mu(E)$, especially at the low-energy and high-energy ends of a spectrum. The XANES at the low-energy end, especially in the presence of a large 'white line', may not be followed well using this Fourier-based approach. Since the EXAFS below 2 Å^{-1} is rarely useful as EXAFS, this is generally not a concern. At the high-energy side, the divergence of the spline for $\mu_0(E)$ away from the $\mu(E)$ data can be appreciable, as can be seen in Fig. 2 for $R_{\rm bkg}$ = 0.2. In extreme cases this can cause problems in subsequent analysis, but it can also be readily accommodated by adding a penalty to the optimization procedure proportional to the difference of $\mu_0(E)$ and $\mu(E)$ at the few highest energy points.

It should be noted that while the presentation here describes the fit for the background and the subsequent analysis of $\chi(k)$ as completely separate steps, this need not always be the case. A spline function that models or refines the low-R components of $\chi(k)$ can be included in the fit of the experimental $\chi(k)$. Indeed, refining the background and structural parameters together in this way can help to illuminate the correlations between parameters describing the background and those describing the structure, and so lead to improved estimates of the values and uncertainties of structural parameters. This capability is available in some analysis packages.

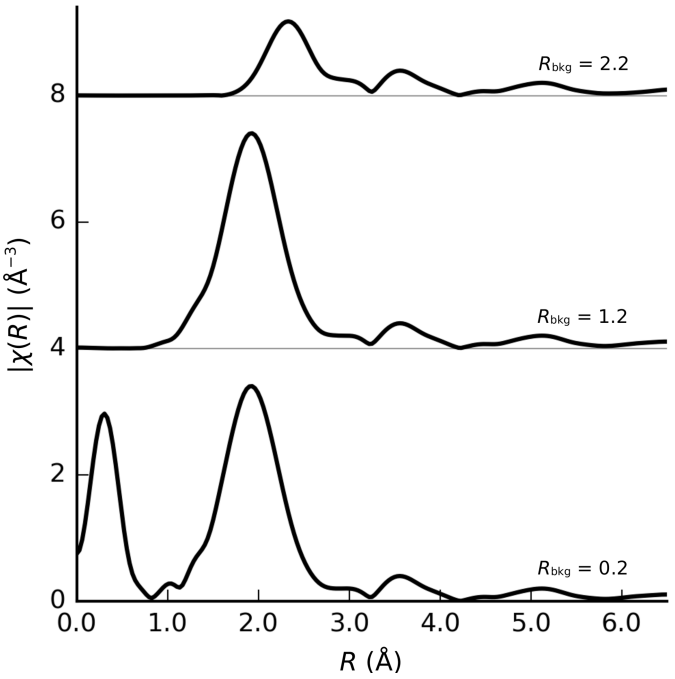

Figure 3
The resulting $|\chi(R)|$ for the NiS_x EXAFS spectrum using $R_{\rm bkg}$ of 0.2, 1.2 and 2.2 Å. The $k^2\chi(k)$ spectra shown in Fig. 2 were Fourier transformed between k = 2.5 and 13.5 Å^{-1} using a Kaiser–Bessel window function.

3. Limitations of the method

While the approach described here for separating the measured $\mu(E)$ into $\mu_0(E)$ and $\chi(k)$ uses physical and mathematical principles, it does rely on the assumption that the EXAFS can be separated from $\mu_0(E)$ based only on the oscillatory properties of the signal. That is, the method essentially asserts that there are no sharp features in $\mu(E)$ other than those caused by EXAFS. Importantly, this ignores multi-electron excitations that can happen within the absorbing atom and give relatively small but sharp steps in $\mu(E)$ that can mimic the main absorption-edge jump. These effects (Li *et al.*, 1992; D'Angelo *et al.*, 1993) are not universally observed but can be appreciable in some spectra. Fortunately, the energies of these excitations can be predicted accurately from the known electronic levels and tend to be within the first few hundred electronvolts above the main edge. The effects of these excitations can be accounted for (Filipponi, 1995), at least partially, by adding a small, broadened step function at the observed excitation energy to the spline function approximating $\mu_0(E)$. Since these excitations tend to be small, they are most noticeable in spectra from gas-phase molecules or highly disordered structures, where the EXAFS is relatively weak. For systems with relatively strong EXAFS, these excitations tend to give a signal that is relatively broad in R-space, so that even an imperfect modelling of these multi-electron peaks tends to be helpful in mitigating their effect on the final structural analysis of $\chi(k)$.

Of course, other sources of sharp features can affect experimental EXAFS measurements, including the absorption edges of other elements, imperfect cancellation of the effects of higher order Bragg peaks or glitches from monochromator crystals, or Bragg diffraction peaks from the sample. Ideally, these systematic errors can be mitigated, but this is not always possible. As with multi-electron excitations, these effects may give features with a very limited energy range for a particular spectrum, although unlike multi-electron excitations they may not necessarily be small or at energies that are predictable from atomic physics. Still, the same type of procedures that are useful for removing multi-electron excitations in the background-removal process may also be useful for removing these experimental artefacts.

Finally, it should be noted that the approach here of separating μ into an atomic-like $\mu_0(E)$ that contains no structural information and $\chi(k)$ that contains all of the structural information does allow some low-R oscillation in $\mu_0(E)$ that may be chemical in nature. Furthermore, since the limited k-range of real EXAFS data means that overlaps in R-space are inevitable, there may be some observable oscillations in $\mu_0(E)$. Whether these can be described as so-called 'atomic XAFS' (Rehr *et al.*, 1994; Ramaker *et al.*, 1999) and

what those oscillations might mean is a topic outside the scope of this chapter and is left for further study.

References

Cook, J. W. Jr & Sayers, D. E. (1981). *J. Appl. Phys.* **52**, 5024–5031.
Boor, C. de (1978). *A Practical Guide to Splines.* New York: Springer-Verlag.
D'Angelo, P., Di Cicco, A., Filipponi, A. & Pavel, N. (1993). *Phys. Rev. A*, **47**, 2055–2063.
Dylan, B. (1971). *When I Paint My Masterpiece.* Big Sky Music.
Filipponi, A. (1995). *Physica B*, **208–209**, 29–32.
Li, G., Bridges, F. & Brown, G. S. (1992). *Phys. Rev. Lett.* **68**, 1609–1612.
Newville, M. (2024). *Int. Tables Crystallogr. I*, ch. 5.13, 690–694.
Newville, M., Līviņš, P., Yacoby, Y., Rehr, J. J. & Stern, E. A. (1993). *Phys. Rev. B*, **47**, 14126–14131.
Ramaker, D., Qian, X. & O'Grady, W. (1999). *Chem. Phys. Lett.* **299**, 221–226.
Rehr, J. J., Booth, C. H., Bridges, F. & Zabinsky, S. I. (1994). *Phys. Rev. B*, **49**, 12347–12350.
Shannon, C. E. (1949). *Proc. IRE*, **37**, 10–21.
Stern, E. A. (1993). *Phys. Rev. B*, **48**, 9825–9827.
Webb, S. M. (2024). *Int. Tables Crystallogr. I*, ch. 5.16, 705–708.